Supporting Information

Sn doped 1T-2H MoS$_2$ few-layer structure embedded in N/P co-doped bio-carbon for high performance sodium-ion batteries

Lingxing Zeng[a, c, e], Fenqiang Luo[a], Xinshu Xia[a], Min-Quan Yang[a], Lihong Xu[a], Jianbiao Wang[b], Xiaoshan Feng[a], Qingrong Qian[*a, c, e], Mingdeng Wei[b], and Qinghua Chen[*a, d, e]

a Engineering Research Center of Polymer Green Recycling of Ministry of Education, College of Environmental Science and Engineering, Fujian Normal University, Fuzhou, Fujian 350007, China. EMAIL: qrqian@fjnu.edu.cn; cqhuar@126.com; Tel: +86-591-83465156
b Institute of Advanced Energy Materials, Fuzhou University, Fuzhou, Fujian 350002, China.
c Fujian Key Laboratory of Pollution Control & Resource Reuse, Fuzhou, Fujian 350007, China.
d Fuqing Branch of Fujian Normal University, Fuqing, Fujian 350300, China.
e Chemistry Post-Doctoral Station, Fujian Normal University, Fuzhou, Fujian 35007, China.

Experimental

Sample preparation

The TH-MoS$_2$-2 was synthesized through a facile one-pot calcination. Firstly, 200 mg of chlorella, 400 mg of phosphomolybdic acid (PMA) and 100 mg of stannous sulfate was added into 40 ml DI water stirring for 24 h. Then the solution was centrifuged and dried at 80 °C. Finally, the green solid was ground with sulfur (w:w=1:2) and calcined at 600 °C (5% H$_2$/95% Ar atmosphere) for 1 h. As a comparison, the H-MoS$_2$-0 was synthesized through the same process by adding 200 mg of chlorella and 500 mg of phosphomolybdic acid (PMA), without adding stannous sulfate. The other two samples were synthesized through the same process by adding 200 mg of chlorella except for the different contents of PMA and stannous sulphate (450 mg of PMA and 50 mg of stannous sulphate denoted as TH-MoS$_2$-1, 350 mg of PMA and 150 mg of stannous sulphate denoted as TH-MoS$_2$-3).

Characterization

The crystal structures of the powders were investigated by XRD (Bruker D8 diffractometer) with Cu-Kα radiation. The microstructures of the powders were performed on SEM (Hitachi 8100) and TEM (FEI F20 S-TWIN). The X-ray photoelectron spectra (XPS) were detected by an ESCALAB MARK II spherical analyzer. Raman (DXR2xi) were performed with a laser at wavelength of 532 nm. The Agilent 725 ICP-OES was used to confirm the ratios of Mo/Sn elements. The CHNSO elemental analysis was measured by an elemntal analyzer (Elementar vario EL cube).

Electrochemical measurements

The active materials (80%), super P (10%) and CMC (10%) were mixed with Di water, followed by spread onto a copper foil to prepare the working electrode. CR2025 coin cells were assembled in glovebox. The amount of active material in test cells was ca. 1–2 mg. The area of work electrode was about 1.1 cm^2. Sodium foil used as counter electrode. The electrolyte is 1 M NaClO$_4$ in 1:1 (weight ratio) EC/PC with 5% fluoroethylene carbonate (FEC) additive. Cyclic performance were carried out within 0.01-3.00 V at room temperature on Land CT 2001A tester with 0.01 voltage range of 0.01-3 V. Cyclic voltammetrys (CV) were analysis at different scan rate. Electrochemical impedance spectroscopy (EIS) was analysis with an Ivium-n-Stat electrochemical workstation from 0.01 Hz to 10000 Hz.
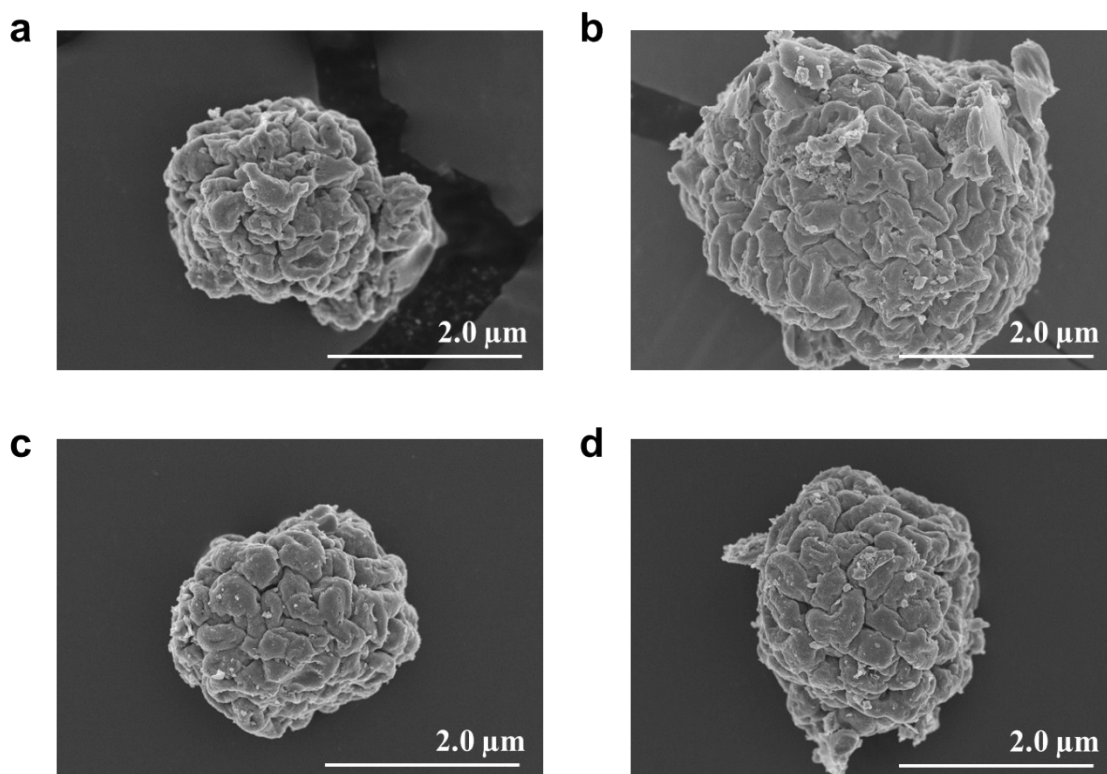
Fig. S1 The SEM images of (a) H-MoS$_2$-0; (b) TH-MoS$_2$-1; (c) TH-MoS$_2$-2 and (d) TH-MoS$_2$-3.
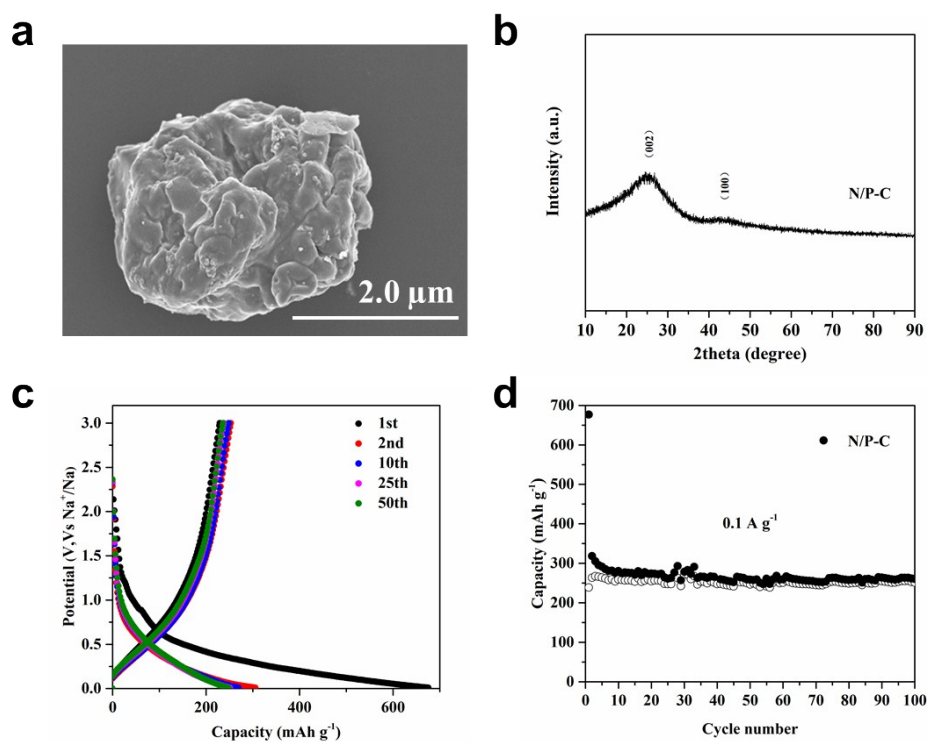

Fig. S2 The (a) SEM image and (b) XRD pattern of pure bio-carbon. The (c) charge-discharge profiles and (d) cycling performance of pure bio-carbon electrode at 0.1 A g^{-1} after 100 cycles in SIBs.
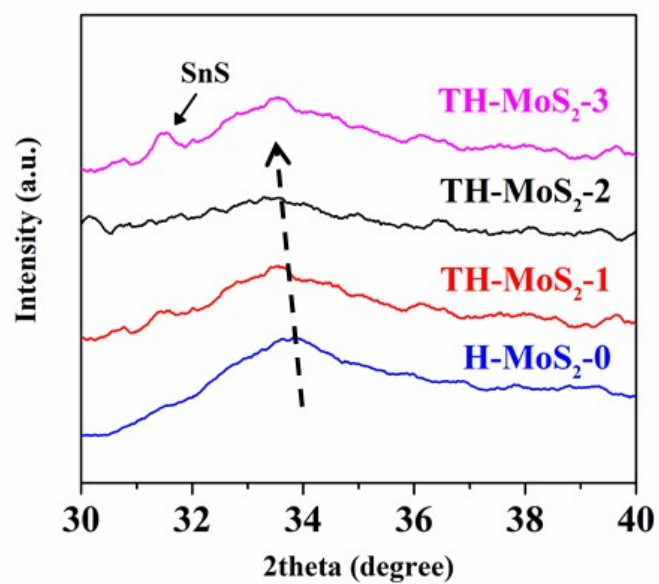
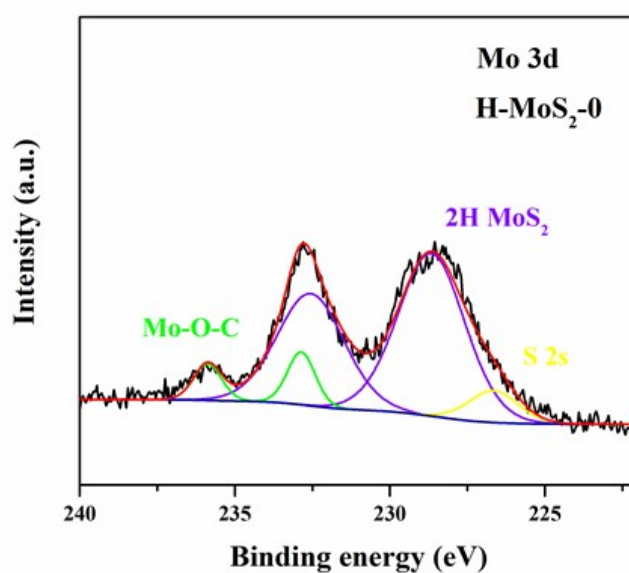**Fig. S3** The enlarged image of XRD pattern of as prepared samples.

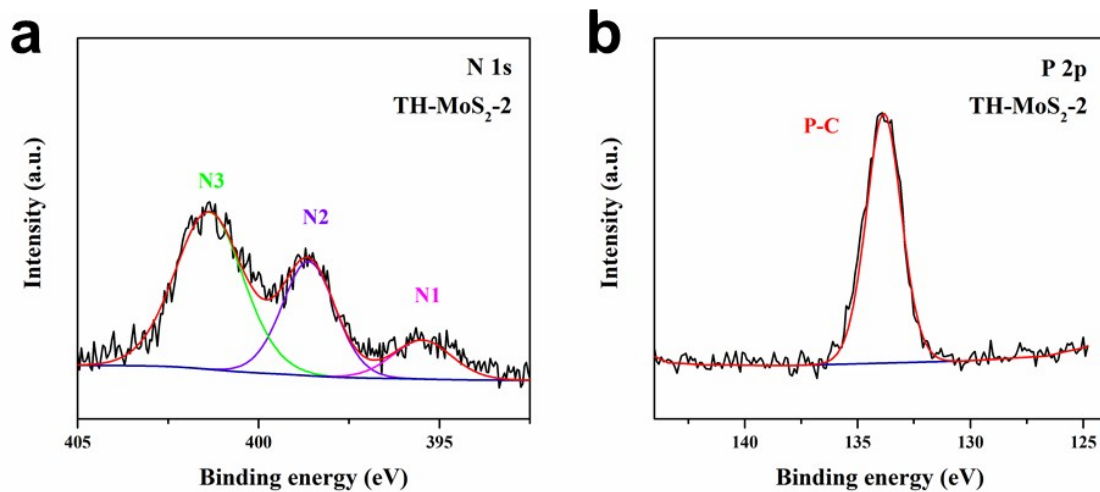**Fig. S4** High-resolution XPS spectrum for H-MoS$_2$-0 sample of Mo 3d.

Fig. S5 High-resolution XPS spectrum for TH-MoS$_2$-2 sample of (a) N 1s and (b) P 2p.
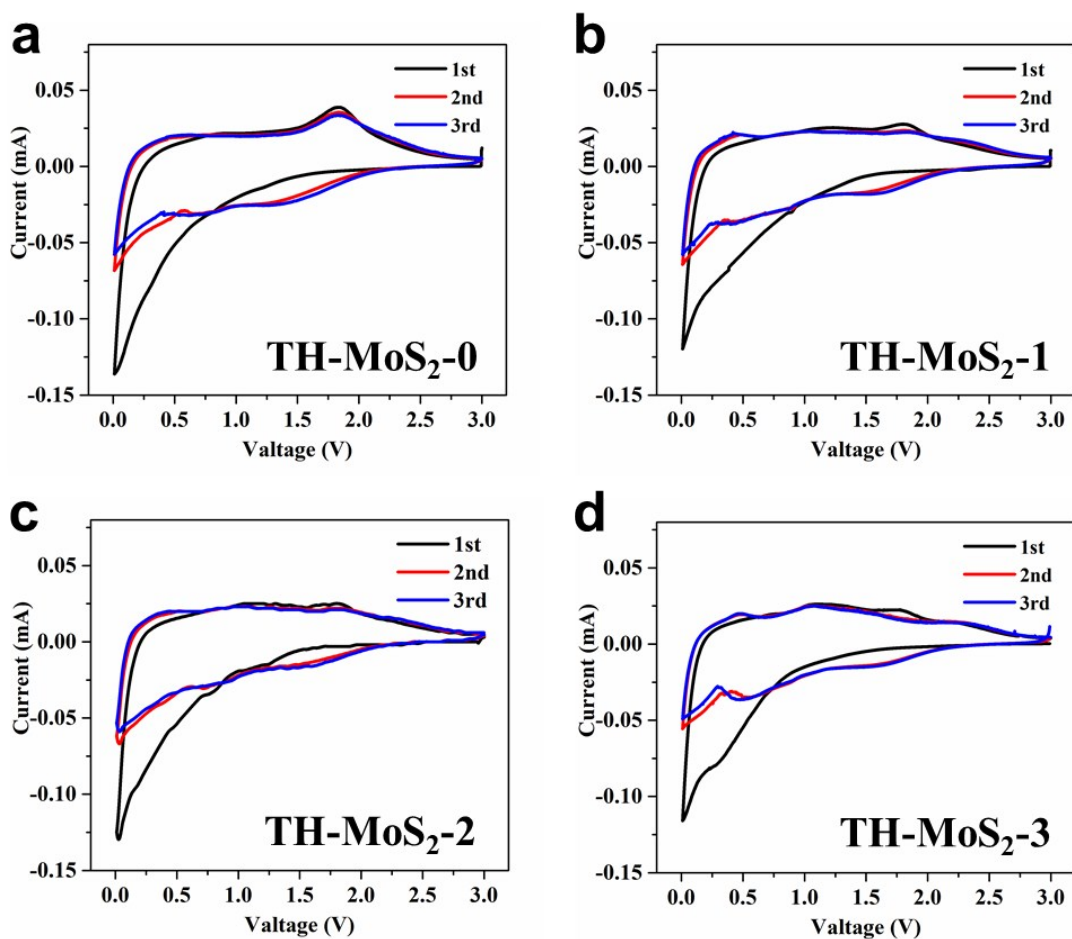

Fig. S6 Cyclic voltammetry curves of (a) H-MoS$_2$-0, (b) TH-MoS$_2$-1, (c) TH-MoS$_2$-2 and (d) TH-MoS$_2$-3 at a scan rate of 0.1 mV s^{-1}.
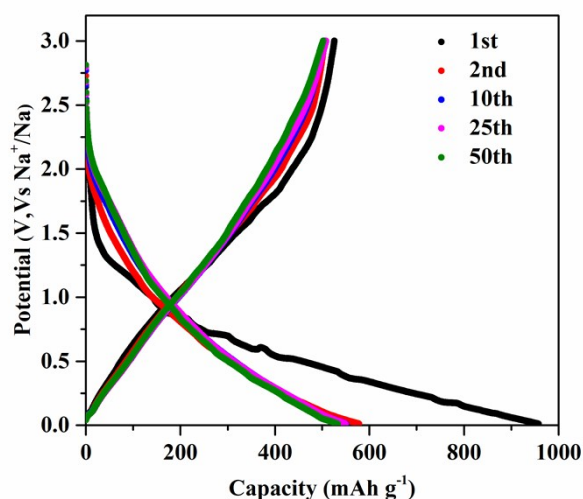
Fig. S7 The charge-discharge profile of TH-MoS$_2$-2 at current density of 0.1 A g^{-1} between 0.01 and 3.0 V for SIBs.
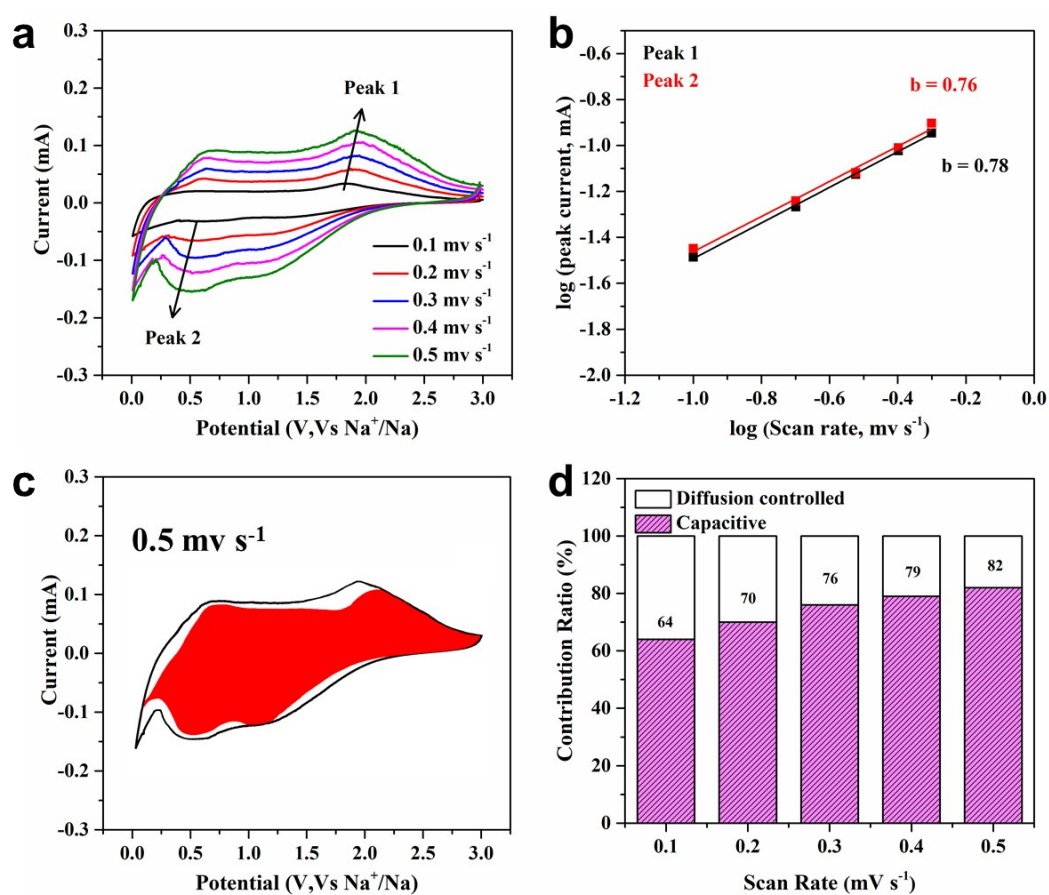

Fig. S8 (a) Cyclic voltammetry curves of H-MoS$_2$-0 electrode at different scan rates from 0.1 to 0.5 mV s^{-1}; (b) log(i) versus log(v) plots at different oxidation and reduction peaks; (c) Capacitive contribution (red area) of TH-MoS$_2$-0 at 0.5 mV s^{-1}; (d) The diffusion controlled (white) and capacitive (pink) capacities of TH-MoS$_2$-0 at different scan rates.
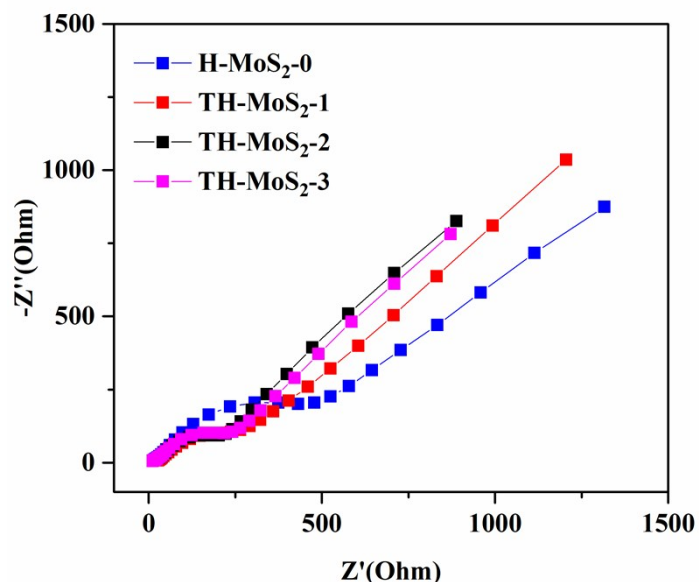
Fig. S9 Electrochemical impedance spectra (EIS) of H-MoS$_2$-0, TH-MoS$_2$-1, TH-MoS$_2$-2 and TH-MoS$_2$-3 electrodes after 50 cycles at 100 mA g^{-1}.
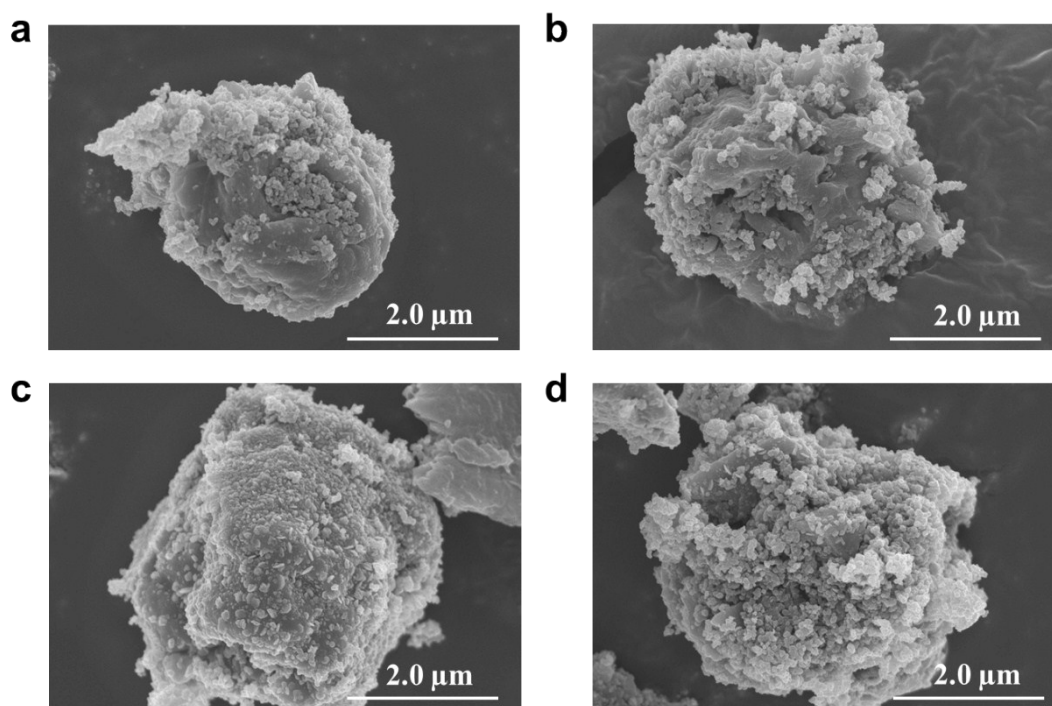

Fig. S10 The SEM images of (a) H-MoS$_2$-0, (b) TH-MoS$_2$-1, (c) TH-MoS$_2$-2 and (d) TH-MoS$_2$-3 electrodes after 50 cycles at 100 mA g^{-1}.

Notes and references

S1. Z. H. Zhao, X. D. Hu, H. Wang, M. Y. Ye, Z. Y. Sang, H. M. Ji, X. L. Li and Y. Dai, *Nano Energy*, 2018, **48**, 526-535.

S2. X. Li, J. Li, Q. Gao, X. Yu, R. Hu, J. Liu, L. Yang and M. Zhu, *Electrochim. Acta*, 2017, **254**, 172-180.

S3. X. Li, Y. Yang, J. W. Liu, L. Z. Ouyang, J. Liu, R. Z. Hu, L. C. Yang and M. Zhu, *Appi. Surf. Sci.*, 2017, **413**, 169-174.

S4. W. Ren, H. Zhang, C. Guan and C. Cheng, *Adv. Funct. Mater.*, 2017, **27**, 1702116.

S5. Y.Q. Teng, H. Zhao, Z. Zhang, L. Zhao, Y. Zhang, Z. Li, Q. Xia, Z. Du and K. Świerczek, *Carbon*, 2017, **119**, 91-100.

S6. B. B. Wang, Y. Xia, G. Wang, Y. X. Zhou and H. Wang, *Chem. Eng. J.*, 2018, **309**, 417-425.

S7. J. X. Wu, Z. H. Lu, K. K. Li, J. Cui, S. S. Yao, M. I. Haq, B. H. Li, Q. H. Yang, F. Y. Kang, C. Francesco and J.-K. Kim, *J. Mater. Chem. A*, 2018, **6**, 5668-5677.

S8.   W. J. Tang, X. L. Wang, D. Xie, X. H. Xia, C. D. Gu and J. P. Tu, *J.Mater. Chem. A*, 2018, **6**, 18318-18324.

S9.   P. Zhang, F. R. Qin, L. Zou, M. R. Wang, K. Zhang, Y. Q. Lai and J. Li, *Nanoscale*, 2017, **9**, 12189-12195.